Why are there so many flatfishes? Jaw asymmetry, diet, and diversification in the Pleuronectiformes

Jonathan Chang[1]

Functional Morphology and Ecology of Fishes
Summer 2014

[1]Department of Ecology and Evolutionary Biology, University of California, Los Angeles, CA 90095, USA.

Contact information:
Jonathan Chang
610 Charles E. Young Drive S
Los Angeles CA 90095
jonathan.chang@ucla.edu

Keywords: flatfish, Pleuronectidae, Paralichthyidae, Bothidae, asymmetry, geometric morphometrics, comparative methods, functional morphology

Abstract
Flatfishes (Actinopterygii: Pleuronectiformes) are a diverse group of teleost fishes, with over 700 species in the order. Jaw asymmetry and diet have been thought to contribute to flatfish diversity but this has not yet been tested in a comparative framework. Here I use geometric morphometric and comparative methods to test whether ocular-blind side asymmetry in flatfish head morphology contributed to flatfish diversification. I find that the repeated convergent evolution of similar morphology, jaw function, and diet likely contribute to the high diversity of flatfishes.

Introduction
Pleuronectiform fishes are highly diverse, with over 700 described species (Froese and Pauly, 2014). These fishes are characterized by their unique bilateral asymmetry and their benthic ecology. Flatfishes also generally consume one of three main types of prey: buried infauna, pelagic fishes and crustaceans, and a third type intermediate to the first two (de Groot 1971, Tsuruta & Omori 1976). I hypothesize that this specialization into different prey types has driven the diversification and morphological disparity in asymmetry of flatfish species.

Methods
12 species of flatfish comprising of 11 genera and 2 families (**Table 1**) were collected via trawl and seine at these sites: Jackson Beach, [48°31'13.0"N 123°00'35.1"W] and Orcas – Eastsound [48°38'26.9"N 122°52'14.0"W]. Specimens that died during capture were frozen for later use, while live specimens were kept in a flow-through tank system at 12°C. All live animal care was in accordance with UW Animal Care protocol #4238-03.

I sacrificed live specimens with a lethal dose (0.5g/L) of Tricaine mesylate (MS-222) buffered to neutral pH with sodium bicarbonate. After 15 minutes in solution and no observed respiratory or opercular movement, I froze the individual at −20°C for later dissection.

For each specimen, I manually opened the jaw to its widest extent and measured its gape height, gape width, and photographed the ventral aspect of the head. I used ImageJ (Rasband, 1997) to measure the angle of jaw deflection to the blind side as described in Gibb (1995). I also measured the standard length and head length of each fish and photographed its external morphology on the ocular side. I approximated cross-sectional gape area assuming that gape height and gape width corresponded to the major (a) and minor (b) axes of an ellipse with the area $A = \pi a b$.

I dissected the head of each specimen, removing the portions of the body caudal to the foramen magnum and operculum (including the pectoral girdle), as well as the gill arches. I removed the eyes, skin, and muscle and stained the remaining bone and connective tissue for one hour with a solution of Alizarin red dye and 0.5% potassium hydroxide (KOH). The head was rinsed in reverse osmosis water and destained for 24 hours in a solution of 0.5% KOH that was changed every 8 hours.

For larger specimens, I photographed the ocular and blind side of the head using a Canon EOS 5D Mark III with a Canon EF 100mm f/2.8 Macro USM lens, with the subject transilluminated on a LightPad A930 (ArtoGraph Inc, Delano, MN). Multiple long (3-8 sec) exposures were automatically combined in Adobe Photoshop to minimize artifacts due to over or underexposure.

I placed homologous landmarks (**Figure 1**) on the opercular and blind side of each specimen using the web-based *mturk-landmark* software (Chang, github.com/jonchang/eol-mturk-landmark). Justification for the selected landmarks are described in Frederich (2008). Data were unpacked using the R package *rjson* (Couture-Beil 2014).

I used a generalized Procustes transform (Rohlf and Slice, 1990) to correct for rotation and scaling, and did principal components analysis (PCA) to determine the largest axes of shape variation in the flatfish head. All geometric morphometric analyses were done in R using the package *geomorph* (Adams and Otarola-Castillo 2013). I also projected diet, gape area, and degree of lateral jaw flexion onto the first two principal components to examine the relationship between head morphology, diet, and jaw function.

I estimated the rate of phenotypic diversification with a recently published phylogeny (Betancur-R 2013) and the R packages *geiger* and *phytools* (Harmon et al 2008, Revell 2012). I projected the phylogeny onto the PCA morphospace previously inferred and examined the relationship between morphology and phylogeny, and also simulated 1000 trees using the SIMMAP algorithm to estimate the rates of transition between infaunal and pelagic feeding types.

Results

The external and jaw measurements of the 13 species sampled are listed in **Table 1**. Standard lengths ranged from 14.1 cm (*Asteresthes stomias*) to 30.4 (*Platichthys stellatus*). The average standard length was 25.2 cm. Gape area ranged from 1 cm^2 (*Microstomus pacificus*) to 81.6 cm^2 (*Hippoglossoides elassodon*), with an average of 14.91 cm^2. Degree of lateral jaw flexion ranged from 1° (*Hippoglossoides elassodon*) to 35° (*Isopsetta isolepis*) with an average lateral flexion of 16.5°.

The thin plate spline analysis (**Figure 2**) showed the major areas of variation among the landmarks sampled. The most variation occurred near the quadratomandibular joint and the insertion of the articular onto the dentary, as well as the length of the maxilla and premaxilla. Smaller amounts of variation occurred on the various neurocranial landmarks.

Projecting the diet and jaw function of the study organisms onto the first two principal components of morphospace revealed a sharp divide between infaunal and pelagic feeders (**Figure 3**). Additionally, jaw functional traits mapped onto the morphospace also showed a similar divide between the infaunal and pelagic feeding types.

Projecting the phylogeny of flatfishes as described in Betancur-R (2013) onto the morphospace showed repeated convergent evolution between the infaunal and pelagic

feeding types (**Figure 4**). Simulating historical diet types also showed frequent transitions (average 3.7 transitions per million years, **Figure 5**) between the two modes of feeding.

Discussion

I have shown that there has been repeated convergent evolution onto similar function and phenotype in these flatfishes, with varying morphology. For example, the two *Citharichthys* species occupy a distinctly different region of morphospace than all other pelagic feeders, yet they lie on the same functional isocline. This implies that there are multiple morphologies that correspond to the same functional outcome, a many-to-one mapping that has been hypothesized to produce large amounts of morphological disparity in other groups of fishes (Wainwright et al 2005, Alfaro et al 2005). Also, the high inferred rate of transition between pelagic and infaunal feeding types show that diet shifts are quite frequent. Combined, these two results suggest that repeated convergent evolution of jaw asymmetry between the pelagic and infaunal feeding types plays a key role in flatfish diversity.

Acknowledgements

I thank Adam Summers, Alice Gibb, Bruno Frédérich, and Matt McGee for invaluable morphometrics, dissection, and specimen preparation advice; Misty Paig-Tran, Stacy Farina, Stephanie Crofts, Nick Gidmark, and Pat Hernandez for helpful discussion; Jacob Harrison and Ian MacDonald for helping with fish identification; the summer 2014 students in the UW Friday Harbor Labs Fish Morphology course and NSF REU program for multiple seine collection expeditions; the crew of the R/V Centennial for trawling collection; and Dexter Summers for fish care. All live animal care and euthanasia was performed according to UW #4238-03. This work was supported by an Encyclopedia of Life Rubenstein Fellowship and a Wainwright Fellowship.

References

Adams, D.C., and E. Otarola-Castillo. 2013. geomorph: an R package for the collection and analysis of geometric morphometric shape data. Methods in Ecology and Evolution. 4:393-399.

Alfaro, M. E., D. I. Bolnick and P. C. Wainwright. 2005. Evolutionary consequences of many-to-one mapping of jaw morphology to mechanics in labrid fishes. American Naturalist 165(6): E140-E154.

Couture-Beil, Alex (2014). rjson: JSON for R. R package version 0.2.14. http://cran.r-project.org/package=rjson

Frédérich B., Adriaens D., Vandewalle P. 2008. Ontogenic shape changes in Pomacentridae (Teleostei, Perciformes) and their relationships with feeding strategies : a geometric morphometric approach. Biological Journal of the Linnean Society 95: 92-105.

Froese, R. and D. Pauly. Editors. 2014. FishBase. www.fishbase.org, version (06/2014).
Gibb, A.C. 1995. Kinematics of prey capture in a flatfish, Pleuronichthys verticalis. J. exp. Biol. 198:1173-1183

Gibson, R. 2005. *Flatfishes: Biology and Exploitation*. Wiley-Blackwell.

Harmon Luke J, Jason T Weir, Chad D Brock, Richard E Glor, and Wendell Challenger. 2008. GEIGER: investigating evolutionary radiations. Bioinformatics 24:129-131.

Rasband, W.S., ImageJ, U. S. National Institutes of Health, Bethesda, Maryland, USA, http://imagej.nih.gov/ij/, 1997-2014.

Revell, L. J. (2012) phytools: An R package for phylogenetic comparative biology (and other things). Methods Ecol. Evol. 3 217-223.

Rohlf, F. J., and D. E. Slice. 1990. Extensions of the Procrustes method for the optimal superimposition of landmarks. Syst. Zool. 39:40-59.

Wainwright, P. C., M. Alfaro, D. I. Bolnick and C. D. Hulsey. 2005. Many-to-one mapping of form to function: a general principle in organismal design? Integrative and Comparative Biology 45(2): 256-262.

Yazdani, G. M. (1969). Adaptations in the jaws of flatfish (Pleuronectiformes). J. Zool., Lond. 159, 181–222.

Figures and Tables

Table 1 - Species collected, measurements of external and jaw morphology, and diet from Gibson (2005).

Species	Standard length	Gape height	Gape width	Jaw angle	Diet type
Atheresthes stomias	14.1 cm	3 cm	1.1 cm	27°	unknown
Citharichthys sordidus	28.6	3.9	2.4	3	pelagic
Citharichthys stigmaeus	25	3.7	2.4	13	pelagic
Eopsetta jordani	28.8	4.4	2.8	18	pelagic
Hippoglossoides elassodon	27.8	5.2	5	1	pelagic
Isopsetta isolepis	21.8	1.7	1.4	35	infaunal
Lepidopsetta bilineata	28.5	2.1	1.9	13	infaunal
Lyopsetta exilis	32	1	1	24	infaunal
Microstomus pacificus	15.8	0.8	0.4	21	infaunal
Parophrys vetulus	30.2	2.6	1.9	30	infaunal
Platichthys stellatus	30.4	2.4	1.9	29	infaunal
Psettichthys melanostictus	19.6	2.1	2	15	pelagic

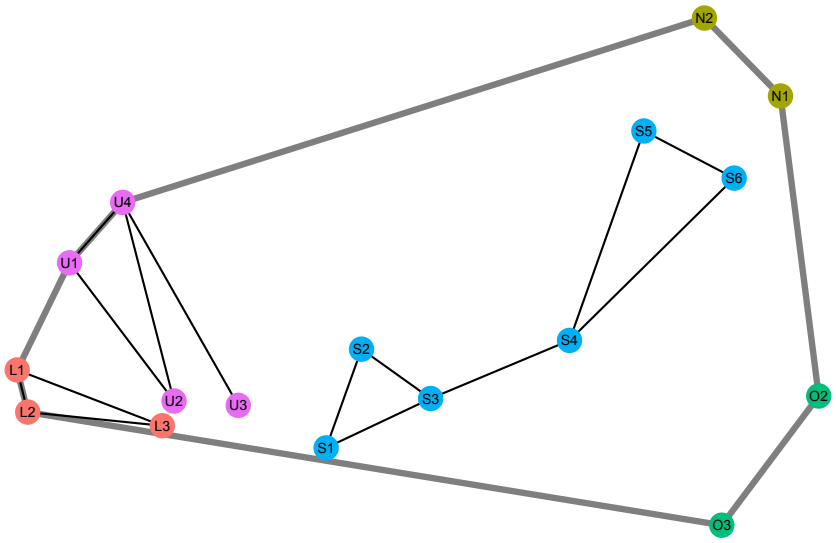

Figure 1 - Landmarks used to digitize head shape. L1: Rostral tip of the dentary. L2: Ventral tip of the dentary. L3: Anterior point of the articular. U1: Anterior tip of the premaxilla. U2: Ventral tip of the premaxilla. U3: Postero-ventral tip of the maxilla. U4: Posterior tip of the ascending process of the premaxilla. S1: Quadratomandibular joint. S2: Intersectino of the quadrate with the ectoptergoid. S3: Intersection of the quadrate with the sympletic. S4: Ventral tip of the hyomandibular. S5: Insertion of the hyomandibular on the pterotic ("suspension point"). S6. Insertion of the opercule and the hyomandibular. O2: Insertion of the opercule on the subopercule. O3: Postero-ventral tip of the interopercule (intersection with the subopercule). N1: Posterior point of the pterotic. N2: Postero-dorsal tip of the epipterotic.

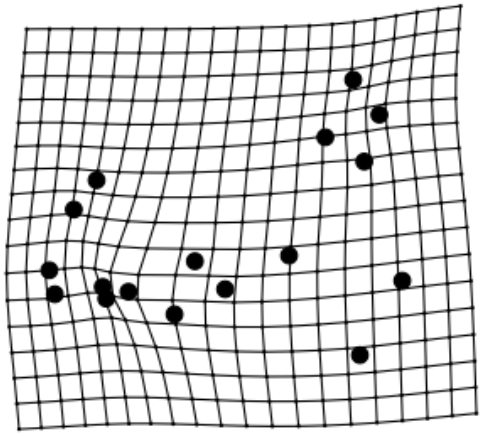

Figure 2 - Thin plate spline analysis for the full landmark set. The most variable landmarks will have the most deformation of the thin plate spline grid, indicating areas of high shape variability among species.

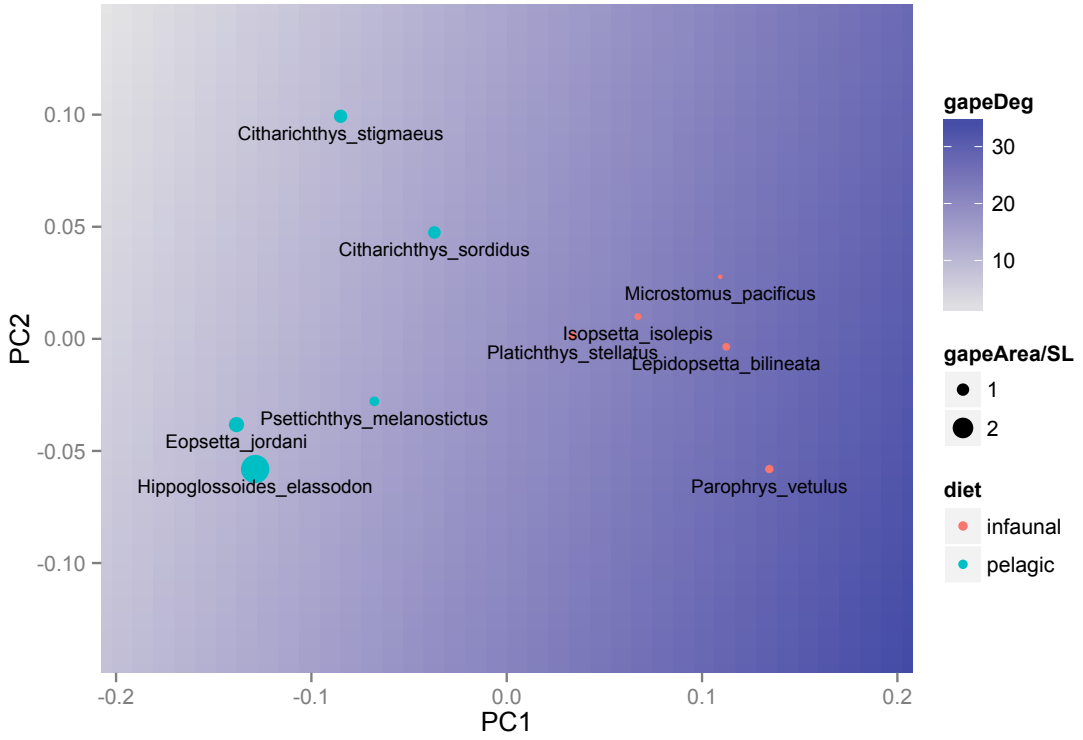

Figure 3 - Morphospace generated by principal components analysis. Together, PC1 and PC2 explain 82% of shape diversity in this data set. Each point represents a species, color represents diet type, size of the point represents gape area corrected by standard length, and background color is the interpolated lateral jaw flexion angle.

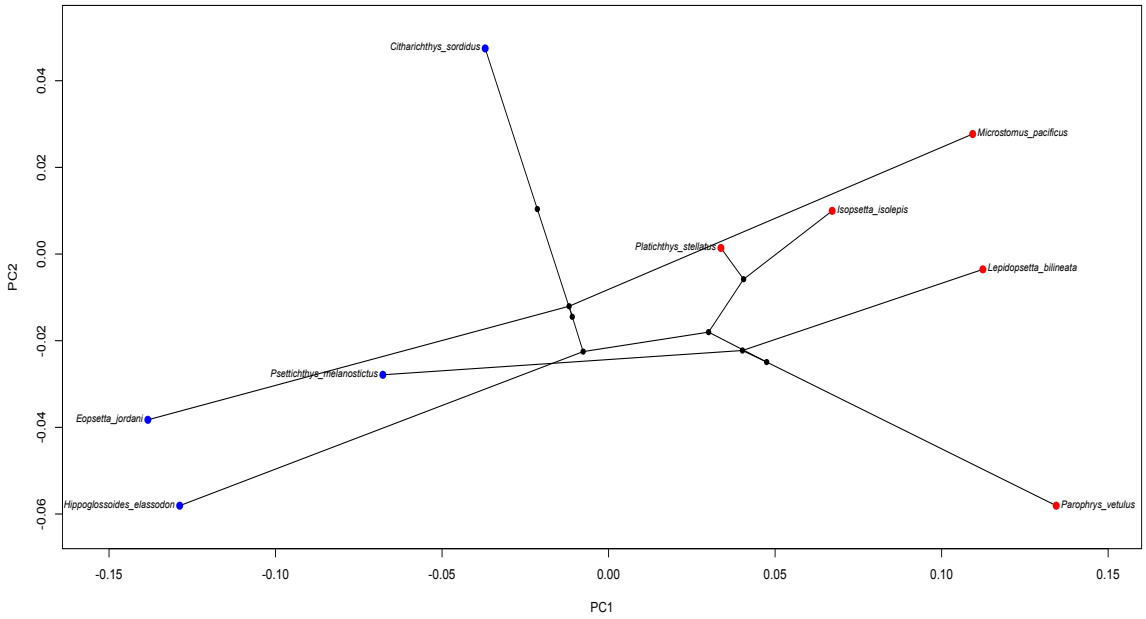

Figure 4 - Projection of the phylogeny from Betancur-R (2013) onto the morphospace. Location of nodes was inferred using a fast Brownian motion simluation technique described in Revell (2012).

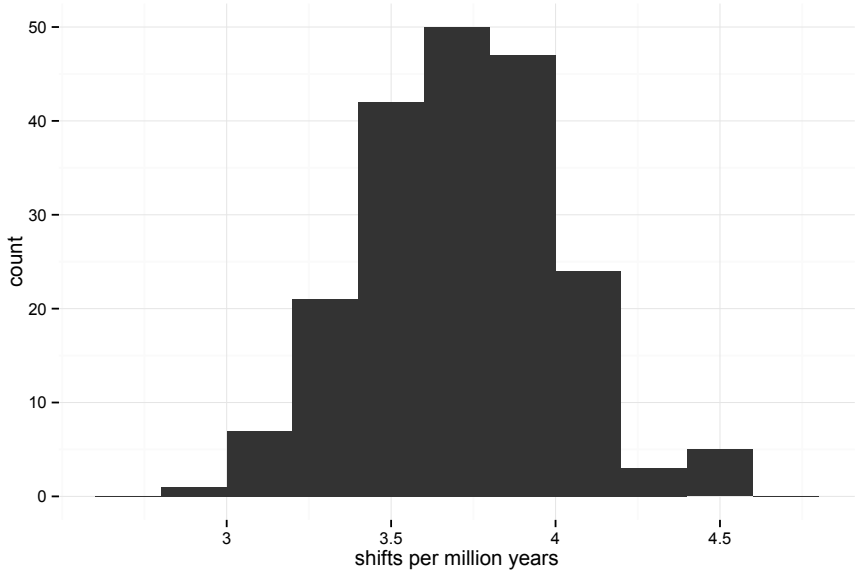

Figure 5 - Histogram of the number of transitions per million years between feeding types on 1000 simulated trees.